

Broken Generalized Kohn Theorem in Harmonic Dot Lattices due to Coulomb Interaction between the Dots: Exact solution of the Schrödinger equation in the dipole approximation

by M. Taut

Institute for Solid State and Materials Research Dresden
 POB 270016, 01171 Dresden, Germany
 email: m.taut@ifw-dresden.de

The Generalized Kohn Theorem in arrays of parabolic quantum dots with Coulomb interaction between the dots is violated, if there are different dot species involved. We solve the Schrödinger equation for cubic lattices with two different dots per unit cell: i) two different circular dots and ii) two elliptical dots, which are rotated by 90° relative to each other. The interaction between the dots is considered in dipole approximation and long- wavelength excitation spectra including FIR intensities are calculated. The energy spectrum of the first case can be expressed as a superposition of two noninteracting dots with an effective confinement frequency, which includes the effect of dot interaction. Only in the second case a splitting of degenerate absorption lines and an anticrossing occurs, which is a qualitative indication for interdot interaction. If the interaction becomes very strong and if all lattice sites (not necessarily confinement potentials) are equivalent, then the contribution of the dot interaction outweigh possible differences in the confinement potentials and the Kohn Theorem gradually reenters, in the sense that one pair of excitation modes (pseudo Kohn modes) becomes independent of the interaction strength.

PACS: 73.20.D (Quantum dots), 73.20.Mf (Collective Excitations)

I. INTRODUCTION

The Generalized Kohn Theorem¹ (GKTh) plays a crucial role in quantum dot physics with far reaching consequences. It considers interacting electron systems in a harmonic confinement and a constant magnetic field, and it states that excitations by long wavelength radiation are not effected by the electron electron (e e) interaction. This statement applies to arrays of *identical* harmonic dot confinements (with e e interaction between the dots) as well (see Appendix of 2). This does not mean that all excitations are independent of e e interaction, but only the optically active ones (Kohn modes), and it does not mean that e e interaction is not important for the other excitations. However, this fact prevents the e e interaction from being seen and investigated e.g. by far infrared (FIR) spectroscopy. The FIR absorption spectrum of the whole system agrees exactly with the spectrum of a single particle. The GKTh does not hold for arrays of *different* dot confinements, e.g. periodic dot lattices with two different harmonic dot confinements per unit cell². Then, all collective modes are excited by FIR radiation and effected by e e interaction, or in other words, there is no Kohn mode. The calculation and investigation of absorption frequencies and probabilities in the latter case is the subject of this work.

In order to obtain a visual picture, let us first consider a classical model for the Kohn mode for vanishing magnetic field. (This preliminary consideration will be replaced by a rigorous quantum mechanical treatment in the following.) Classically, the charge distributions of all dots oscillate rigidly in- phase with the bare confinement frequency, and the e e interaction contributes only a constant term to the total energy (independent of elongation). If we have more than one *identical* dots per unit cell, there are additional collective modes, in which the individual dots oscillate out of phase, and which are affected by dot interaction, but which are not optically active. Consequently, the dot interaction is not observable with FIR spectroscopy in arrangements of *identical* dots. One way to trick Kohn's theorem is to include *different* dot species. Then, there is no coherent oscillation mode for all dots, which does not change the e e interaction energy of the system in elongation, because there is no common bare confinement frequency. As a consequence, all collective modes (two modes per dot in the unit cell) are effected by dot interaction and excited by FIR radiation with a finite probability. In other words, the Generalized Kohn Theorem for dot arrays is broken. Other systems, where Kohn's Theorem does not hold, comprise: i) anharmonic confinements^{3,4} (circular dots with r^4 and higher order terms in the radial dependence or cubic dots with terms of type $x^2 y^2$), ii) hole dots with different effective masses⁵. One point of this paper is that the GKTh can be broken despite an exactly harmonic Hamiltonian. A further possibility to observe the e e interaction in the excitations is to consider finite wave length^{2,3}.

II. MAGNETOPHONON HAMILTONIAN

The first part of the calculation of the eigenstates of the Hamiltonian follows closely the procedure described in Ref. 2. We only have to consider that *now the confinement potentials and electron numbers can be different* in different dots. After introducing center– of – mass (c.m.) and relative coordinates in each dot and applying the dipole approximation for the Coulomb interaction between the dots, we observe that the Hamiltonian of all c.m. coordinates is decoupled from individual dot Hamiltonians in the relative coordinates. That's why all excitations can be classified into i) collective (c.m.) excitations, and ii) intra-dot excitations. The latter are not considered here because they are not optically active. The Hamiltonian in the c.m. coordinates $\mathbf{R}_{n,\alpha}$ reads in atomic units $\hbar = m = e = 1$ (see also Sect. IV A in Ref. 2)

$$H_{c.m.} = \sum_{n,\alpha} \frac{1}{2m^*} \left[\frac{\mathbf{P}_{n,\alpha}}{\sqrt{N_\alpha}} + \frac{\sqrt{N_\alpha}}{c} \mathbf{A}(\mathbf{U}_{n,\alpha}) \right]^2 + \frac{1}{2} \sum_{\substack{n,\alpha \\ n',\alpha'}} \sqrt{N_\alpha N_{\alpha'}} \mathbf{U}_{n,\alpha} \cdot \mathbf{C}_{n,\alpha; n',\alpha'} \cdot \mathbf{U}_{n',\alpha'} \quad (1)$$

where $\mathbf{U}_{n,\alpha} = \mathbf{R}_{n,\alpha} - \mathbf{R}_{n,\alpha}^{(0)}$ is the elongation of the c.m. at lattice site (n, α) and $\mathbf{P}_{n,\alpha} = -i \nabla_{\mathbf{U}_{n,\alpha}}$ is the corresponding canonical momentum operator. n runs over the unit cells and α over the dot species within a cell. N_α is the number of electrons in dot α , and m^* the effective mass. It is clear already from inspection of (1) that the eigenvalues of $H_{c.m.}$ do not depend on the explicitly shown electron numbers N_α , because the factors $\sqrt{N_\alpha}$ can be considered just as a rescaling factor of the coordinates $\mathbf{U}_{n,\alpha}$. However, the eigenfunctions (and quantities derived from them) do depend on the explicit N_α . The force constant tensor reads

$$C_{n,\alpha; n,\alpha} = \Omega_\alpha + \epsilon^{-1} N_\alpha \sum_{n',\alpha' (\neq n,\alpha)} \mathbf{T} \left(\mathbf{R}_{n,\alpha}^{(0)} - \mathbf{R}_{n',\alpha'}^{(0)} \right) \quad (2)$$

$$C_{n,\alpha; n',\alpha'} = -\epsilon^{-1} \sqrt{N_\alpha N_{\alpha'}} \mathbf{T} \left(\mathbf{R}_{n,\alpha}^{(0)} - \mathbf{R}_{n',\alpha'}^{(0)} \right) \quad \text{for } (n, \alpha) \neq (n', \alpha') \quad (3)$$

where ϵ^{-1} is the inverse background dielectric constant and Ω_α the bare confinement tensor, which produces a harmonic confinement. The dipole tensor is defined as $\mathbf{T}(\mathbf{a}) = \frac{1}{a^5} [3 \mathbf{a} \circ \mathbf{a} - a^2 \mathbf{I}]$ where (\circ) denotes the dyad product and \mathbf{I} the unit tensor. Observe that \mathbf{C} depends on N_α implicitly which effects the energy eigenvalues.

A unitary transformation to collective magnetophonon coordinates

$$\mathbf{U}_{n,\alpha} = \frac{1}{\sqrt{N_c}} \sum_{\mathbf{q}}^{BZ} e^{-i\mathbf{q} \cdot \mathbf{R}_n^{(0)}} \mathbf{U}_{\mathbf{q},\alpha} \quad (4)$$

$$\mathbf{P}_{n,\alpha} = \frac{1}{\sqrt{N_c}} \sum_{\mathbf{q}}^{BZ} e^{+i\mathbf{q} \cdot \mathbf{R}_n^{(0)}} \mathbf{P}_{\mathbf{q},\alpha} \quad (5)$$

where N_c is the number of unit cells, leaves us with a sum on N_c decoupled subsystems $H_{c.m.} = \sum_{\mathbf{q}} H_{\mathbf{q}}$

$$H_{\mathbf{q}} = \sum_{\alpha} \frac{1}{2m^*} \left[\frac{\mathbf{P}_{\mathbf{q},\alpha}}{\sqrt{N_\alpha}} + \frac{\sqrt{N_\alpha}}{c} \mathbf{A}(\mathbf{U}_{\mathbf{q},\alpha}^*) \right]^\dagger \cdot \left[\frac{\mathbf{P}_{\mathbf{q},\alpha}}{\sqrt{N_\alpha}} + \frac{\sqrt{N_\alpha}}{c} \mathbf{A}(\mathbf{U}_{\mathbf{q},\alpha}^*) \right] + \frac{1}{2} \sum_{\alpha,\alpha'} \sqrt{N_\alpha N_{\alpha'}} \mathbf{U}_{\mathbf{q},\alpha}^* \cdot \mathbf{C}_{\mathbf{q};\alpha,\alpha'} \cdot \mathbf{U}_{\mathbf{q},\alpha'} \quad (6)$$

which includes the dynamical matrix

$$\mathbf{C}_{\mathbf{q};\alpha,\alpha'} = \sum_n e^{i\mathbf{q} \cdot \mathbf{R}_n^{(0)}} \mathbf{C}_{\alpha,\alpha'} \left(\mathbf{R}_n^{(0)} \right) ; \quad \mathbf{C}_{\alpha,\alpha'} \left(\mathbf{R}_n^{(0)} \right) = \mathbf{C}_{n,\alpha; 0,\alpha'} \quad (7)$$

With (2) and (3), we obtain

$$C_{\mathbf{q};\alpha,\alpha} = \mathbf{\Omega}_\alpha + \epsilon^{-1} N_\alpha \sum_{\alpha'(\neq\alpha)} \mathbf{T}(\mathbf{a}_\alpha - \mathbf{a}_{\alpha'}) \quad (8)$$

$$+ \sum_{n \neq 0} \left[\sum_{\alpha'} \mathbf{T}(\mathbf{R}_n^{(0)} + \mathbf{a}_\alpha - \mathbf{a}_{\alpha'}) - e^{i\mathbf{q} \cdot \mathbf{R}_n^{(0)}} \mathbf{T}(\mathbf{R}_n^{(0)}) \right] \quad (9)$$

$$C_{\mathbf{q};\alpha,\alpha'} = -\epsilon^{-1} \sqrt{N_\alpha N_{\alpha'}} \sum_n e^{i\mathbf{q} \cdot \mathbf{R}_n^{(0)}} \mathbf{T}(\mathbf{R}_n^{(0)} + \mathbf{a}_\alpha - \mathbf{a}_{\alpha'}) \quad \text{for } \alpha \neq \alpha' \quad (10)$$

where $\mathbf{R}_{n,\alpha}^{(0)} = \mathbf{R}_n^{(0)} + \mathbf{a}_\alpha$ and $n \neq 0$ under the sum means that the term $\mathbf{R}_n^{(0)} = 0$ is excluded.

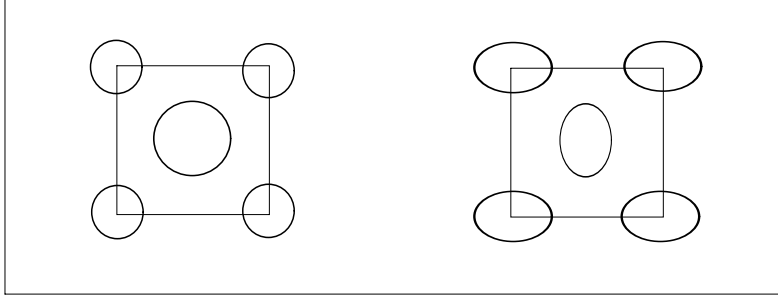


FIG. 1. Minimum unit cells for the two dot architectures considered in this paper with two different circular dots (left) and two identical, but rotated, ellipsoidal dots (right).

Now, we focus our attention to long-wavelength modes (the index $\mathbf{q} = 0$ is dropped henceforth) and consider a simple cubic lattice, alternatively occupied by two different dot species. The minimum unit cell is face centered cubic (see Fig.1) with lattice constant a . After performing the lattice sum involved in (7) numerically, we obtain the four 2×2 dynamical matrices

$$\mathbf{C}_{11} = \mathbf{\Omega}_1 + d p_1 \mathbf{I} \quad (11)$$

$$\mathbf{C}_{22} = \mathbf{\Omega}_2 + d p_2 \mathbf{I} \quad (12)$$

$$\mathbf{C}_{12} = \mathbf{C}_{21} = -d p_{12} \mathbf{I} \quad (13)$$

with the interaction parameters

$$p_i = 2N_i \epsilon^{-1} / (n.n.distance)^3 = 4\sqrt{2} N_i \epsilon^{-1} / a^3, \quad (i = 1, 2) \quad (14)$$

$$p_{12} = 2\sqrt{N_1 N_2} \epsilon^{-1} / (n.n.distance)^3 = 4\sqrt{2} \sqrt{N_1 N_2} \epsilon^{-1} / a^3 \quad (15)$$

and $d = 1.460$. From the preceding definitions it follows that $p_{12} = \sqrt{p_1 p_2}$.

III. EIGENSTATES

Now we are going to find eigenvalues and eigenfunction of (6). For avoiding divergences for $B = 0$, we add an isotropic oscillator potential $\frac{1}{2} \sum_\alpha \omega_0^2 \mathbf{U}_\alpha^2$ to the kinetic energy in (6) and subtract it from the interaction term. ω_0 is

in principle arbitrary, but we chose the mean value of the bare confinement frequencies included in Ω_1 and Ω_2 . Now we replace the coordinates in (6) (for $\mathbf{q} = 0$) by Boson ladder operators. This is analogous to the usual text book transformation (see e.g. Ref. 6 Sect. 3.3) apart from the factors $\sqrt{N_\alpha}$. It is obvious that this modification can be taken into account by introducing scaled coordinates $\mathbf{U}_\alpha \rightarrow \tilde{\mathbf{U}}_\alpha = \sqrt{N_\alpha} \mathbf{U}_\alpha$ (what implies $\mathbf{P}_\alpha \rightarrow \tilde{\mathbf{P}}_\alpha = \mathbf{P}_\alpha / \sqrt{N_\alpha}$).

$$\sqrt{N_\alpha} U_{\alpha x} = \frac{1}{2} \sqrt{\frac{2}{\tilde{\omega}_c^*}} \left(a_{\alpha 1}^+ + a_{\alpha 2}^+ + a_{\alpha 1} + a_{\alpha 2} \right) \quad (16)$$

$$\sqrt{N_\alpha} U_{\alpha y} = -\frac{i}{2} \sqrt{\frac{2}{\tilde{\omega}_c^*}} \left(a_{\alpha 1}^+ - a_{\alpha 2}^+ - a_{\alpha 1} + a_{\alpha 2} \right) \quad (17)$$

where the first subscript ($\alpha = 1, 2$) indicates the dot number and the second one the component. The transformation of the c.m. momentum operators is analogous.

$$\frac{P_{\alpha x}}{\sqrt{N_\alpha}} = \frac{i}{2} \sqrt{\frac{\tilde{\omega}_c^*}{2}} \left(a_{\alpha 1}^+ + a_{\alpha 2}^+ - a_{\alpha 1} - a_{\alpha 2} \right) \quad (18)$$

$$\frac{P_{\alpha y}}{\sqrt{N_\alpha}} = \frac{1}{2} \sqrt{\frac{\tilde{\omega}_c^*}{2}} \left(a_{\alpha 1}^+ - a_{\alpha 2}^+ + a_{\alpha 1} - a_{\alpha 2} \right) \quad (19)$$

The cyclotron frequency is $\omega_c^* = B/m^*c$ and $\tilde{\omega}_c^* = \sqrt{\omega_c^{*2} + 4\omega_0^2}$. Firstly, it is clear that the Hamiltonian in these ladder operators does not show an explicit N_α -dependence anymore (apart from that implicit in the dynamical matrix). This implies that the eigenvalues of the Hamiltonian do not depend on those N_α explicitly seen in (6). Secondly, the commutators of the ladder operators are not influenced by the N_α -factors and agree with those of Bosons: $[a_{\alpha i}, a_{\alpha i}^+] = 1$ and all other commutators vanish. (This is because the commutators of the $\tilde{\mathbf{U}}_\alpha$ and $\tilde{\mathbf{P}}_{\alpha'}$ agree with the commutators of the untilded quantities.) Now, the total Hamiltonian can be written in matrix notation in the following compact form

$$H = [\mathbf{a}^+ \mathbf{a}] \cdot \mathbf{H} \cdot \begin{bmatrix} \mathbf{a} \\ \mathbf{a}^+ \end{bmatrix} \quad (20)$$

where

$$[\mathbf{a}^+ \mathbf{a}] = [a_{11}^+ a_{12}^+ a_{21}^+ a_{22}^+ | a_{11} a_{12} a_{21} a_{22}] \quad (21)$$

and $\begin{bmatrix} \mathbf{a} \\ \mathbf{a}^+ \end{bmatrix}$ is the transposed and Hermitian conjugate of (21). The 8×8 Hamiltonian matrix is not unique, but can be cast into the following form

$$\mathbf{H} = \begin{bmatrix} \alpha & \beta \\ \beta^* & \alpha^* \end{bmatrix} \quad \text{with} \quad \alpha^+ = \alpha ; \quad \beta^T = \beta \quad (22)$$

consisting of the 4×4 matrices

$$\alpha = \frac{1}{2} \begin{bmatrix} \omega & 0 \\ 0 & \omega \end{bmatrix} + \frac{1}{4 \tilde{\omega}_c^*} \mathbf{E}^+ \cdot \begin{bmatrix} \tilde{\mathbf{C}}_{11} & \mathbf{C}_{12} \\ \mathbf{C}_{21} & \tilde{\mathbf{C}}_{22} \end{bmatrix} \cdot \mathbf{E} \quad (23)$$

$$\beta = \frac{1}{4 \tilde{\omega}_c^*} \mathbf{E}^+ \cdot \begin{bmatrix} \tilde{\mathbf{C}}_{11} & \mathbf{C}_{12} \\ \mathbf{C}_{21} & \tilde{\mathbf{C}}_{22} \end{bmatrix} \cdot \mathbf{E}^* \quad (24)$$

with $\mathbf{E} = \begin{bmatrix} \varepsilon & 0 \\ 0 & \varepsilon \end{bmatrix}$ and the 2×2 matrices

$$\tilde{\mathbf{C}}_{kk} = \mathbf{C}_{kk} - \frac{1}{2} \omega_0^2 \mathbf{I} ; \quad \omega = \begin{bmatrix} \omega_+ & 0 \\ 0 & \omega_- \end{bmatrix} ; \quad \varepsilon = \begin{bmatrix} 1 & 1 \\ i & -i \end{bmatrix} \quad (25)$$

with

$$\omega_{\pm} = \sqrt{\omega_o^2 + \left(\frac{\omega_c^*}{2}\right)^2} \pm \left(\frac{\omega_c^*}{2}\right) \quad (26)$$

Finding the eigenstates of the Boson Hamiltonian (20) is provided by mathematical physics and described in Ref. 8 in full detail. The goal is to find a linear transformation $\begin{bmatrix} \mathbf{b} \\ \mathbf{b}^+ \end{bmatrix} = \mathbf{A} \cdot \begin{bmatrix} \mathbf{a} \\ \mathbf{a}^+ \end{bmatrix}$ which preserves Boson commutators and diagonalizes H . We shall only summarize the recipe here.

The eigenvalues are given by $E_{n_1, n_2, n_3, n_4} = \sum_k^{(1\dots 4)} \left(n_k + \frac{1}{2}\right) \omega_k$ with n_k being non-negative integers and $\omega_k = 2 \gamma_k$ with γ_k being the four positive eigenvalues of the matrix $\mathbf{H} \cdot \mathbf{J}$. The 8×8 matrix $\mathbf{J} = \begin{bmatrix} \mathbf{I} & 0 \\ 0 & -\mathbf{I} \end{bmatrix}$ is made up of 4×4 unit matrices. All eigenvalues of $\mathbf{H} \cdot \mathbf{J}$ come in pairs $(\gamma_k, -\gamma_k)$.

The eigenfunctions of H are constructed as usual for Bosons

$$|n_1, n_2, n_3, n_4\rangle = \prod_k^{(1\dots 4)} \frac{\left(b_k^+\right)^{n_k}}{\sqrt{n_k!}} |0\rangle \quad (27)$$

The four eigenvectors belonging to the positive eigenvalues are written in the form $\mathbf{x}_k = \begin{bmatrix} \mathbf{u}_k \\ \mathbf{v}_k \end{bmatrix}$. The column vectors of \mathbf{A}^+ are given by the vectors \mathbf{x}_k , and by the vectors $\hat{\mathbf{x}}_k = \begin{bmatrix} \mathbf{v}_k^* \\ \mathbf{u}_k^* \end{bmatrix}$, which are the eigenvectors belonging to $-\gamma_k$. The eigenvectors have to be properly orthonormalized $\mathbf{x}_i^+ \cdot \mathbf{J} \cdot \mathbf{x}_k = \delta_{i,k}$. Without degeneracy, the orthogonality is guaranteed automatically. The inverse of this particular transformation is obtained from $\mathbf{A}^{-1} = \mathbf{J} \cdot \mathbf{A}^+ \cdot \mathbf{J}$ which shows that the linear transformation is not unitary (but unitary in a non-Euklidian metric).

IV. OSCILLATOR STRENGTH

Optical oscillator strength between the states $|n\rangle = |n_1, n_2, n_3, n_4\rangle$ and $|n'\rangle = |n'_1, n'_2, n'_3, n'_4\rangle$ for polarization in $\eta = (x \text{ or } y)$ direction are defined as

$$f_{n,n';\eta} = 2 m^* \omega_{n,n'} |< n | \mathbf{U}_{\eta;tot} | n' >|^2 \quad (28)$$

where $\omega_{n,n'}$ is the corresponding excitation energy, and $\mathbf{U}_{\eta;tot}$ is the η -component of the total c.m. of the electrons in a unit cell (apart from a constant term). In formulae, this means $\mathbf{U}_{tot} = \frac{N_1}{N_{tot}} \mathbf{U}_1 + \frac{N_2}{N_{tot}} \mathbf{U}_2$, where $N_{tot} = N_1 + N_2$. After expressing the vectors \mathbf{U} by ladder operators b_k, b_k^+ and using (27), we obtain the usual selection rules, i.e., only one quantum with energy ω_k can be absorbed or emitted, so that we obtain only four absorption lines. The result for the oscillator strength for the four possible transitions ($k = 1\dots 4$) and for η -polarization reads

$$f_{k,\eta} = \frac{m^* \omega_k}{N_{tot} \tilde{\omega}_c^*} |S_{k,\eta}|^2 \cdot \begin{cases} (n_k + 1) & \text{for absorption} \\ n_k & \text{for emission} \end{cases} \quad (29)$$

where n_k denotes the initial state, and

$$S_{k,x} = \sum_i^{(1,2)} \sqrt{\frac{N_1}{N_{tot}}} (u_{ki} - v_{ki}) + \sum_i^{(3,4)} \sqrt{\frac{N_2}{N_{tot}}} (u_{ki} - v_{ki}) \quad (30)$$

$$S_{k,y} = \sum_i^{(1,2)} \sqrt{\frac{N_1}{N_{tot}}} (-1)^{(i+1)} (u_{ki} + v_{ki}) + \sum_i^{(3,4)} \sqrt{\frac{N_2}{N_{tot}}} (-1)^{(i+1)} (u_{ki} + v_{ki}) \quad (31)$$

In the last definition, u_{ki} and v_{ki} for $i=1\dots 4$ are the components of the vectors \mathbf{u}_k and \mathbf{v}_k , respectively. The oscillator strength defined in (28) fulfill the following exact f -sum rule $\sum_k f_{k,\eta} = \frac{1}{N_{tot}}$. It is worth pointing out that for equal electron numbers in either dot ($N_1 = N_2 = N$), the oscillator strength depends explicitly on N (contrary to the optical excitation energies). In all figures presented below the oscillator strength are for $N_1 = N_2 = N$.

V. RESULTS

Now the two simplest cases are discussed in more detail: two different circles and two identical, but rotated ellipses. The ratio of the two bare confinement frequencies involved in either case is 1:1.5 which means, that the two confinement frequencies in units of the mean frequency ω_0 are 1.2 and 0.8. In our figures, all frequencies (energies) are given in units of the mean confinement frequency ω_0 and the interaction parameters p in units of ω_0^2 . The magnetic field is given in terms of the effective cyclotron frequency ω_c^* in units of ω_0 (upper scale) and in *Tesla* (lower scale). The conversion between both scales is provided by

$$\omega_c^*[\omega_0] = \frac{0.9134 \cdot 10^{-2}}{m^* \omega_0[a.u.^*]} B[Tesla] \quad (32)$$

In our figures we used $\omega_0 = 0.2 \text{ a.u.}^* = 2.53 \text{ meV}$ and m^* of GaAs for this conversion. (We want to stress that this parameter choice effects only the magnetic field scale and not the curves.) The definitions of the interaction parameters (14) for GaAs in more convenient units reads

$$p_i[\omega_0^2] = \frac{2.26 \cdot 10^7 N_i}{(n.n.distance[\text{\AA}])^3 (\omega_0[\text{meV}])^2} \quad (33)$$

(For a more detailed discussion of order- of – magnitude estimates see Ref. 2.)

For two different *circular dots* with bare confinement frequencies ω_1 and ω_2 and $N_1 = N_2$, the absorption spectrum and the oscillator strength are shown in Fig.2. Although *all* absorption lines are effected by the dot interaction (represented by the interaction parameter p), and *all* modes are optically active, there is no *qualitative* effect of interaction in the position of the absorption lines. The reason can be understood easily. In this particular case, the four eigenmodes can be calculated analytically providing

$$\omega_{1,2,3,4} = \sqrt{\omega_{eff,i}^2 + \left(\frac{\omega_c^*}{2}\right)^2} \pm \left(\frac{\omega_c^*}{2}\right), \quad (i = 1, 2) \quad (34)$$

where

$$\omega_{eff,1,2}^2 = \frac{(\omega_1^2 + \omega_2^2)}{2} + \frac{(p_1 + p_2)}{2} d \pm \sqrt{\left[\frac{(\omega_1^2 + \omega_2^2)}{2} + \frac{(p_1 + p_2)}{2} d\right]^2 - (\omega_1^2 p_2 d + \omega_2^2 p_1 d + \omega_1^2 \omega_2^2)} \quad (35)$$

(The upper and lower sign belongs to $\omega_{eff,1}$ and $\omega_{eff,2}$, respectively). Consequently, if we had to interpret an experimental spectrum, we could do this using the formula (34) for non- interacting dots, but with the effective (i.e. interaction affected) confinement parameters defined in (35). Only if we take the intensities into account, we see some qualitative effect. Whereas for non- interacting dots (with $p = 0$) and for $B = 0$ the oscillator strength of all modes agree (for a single oscillator, f is independent of the oscillator frequency), there is a large difference for interacting dots at $p = 0.5$. This large difference can be understood as follows. In the limit $p \rightarrow \infty$, the upper pair of modes develops into the spurious Brillouin zone boundary mode, which has vanishing oscillator strength and the sum rule has to be fulfilled only by the lower pair (see also the discussion below).

In Fig.2 both dot species bare the same number of electrons. Therefore, only one interaction parameter p is involved. Calculations with different N_i (and p_i) do not show any qualitative difference. In the limit of large p (and equal electron numbers) we obtain from (35)

$$\omega_{eff,1,2}^2 = \frac{(\omega_1^2 + \omega_2^2)}{2} + \left\{ \begin{array}{l} 2 p d \\ 0 \end{array} \right. \pm \frac{(\omega_1^2 - \omega_2^2)}{8 p d} + O(p^{-3}) \quad (36)$$

Consequently, the square of the smaller effective confinement frequency (which is the only one giving rise to modes with a finite oscillator strength for large p) approaches the mean value of both squared bare confinement frequencies, whereas the larger one grows continuously for large p .

In Fig.3 and 4b we show the results for two identical, but mutually rotated, *elliptical dots*. Without dot interaction ($p = 0$), we have two doubly degenerate lines. With increasing interaction strength, we observe a splitting of degenerate modes and an anti-crossing behavior for finite B . As in the case of circular dots, the oscillator strength at $B = 0$ for non- interacting dots ($p = 0$) agree for all four modes. The dot interaction lifts this degeneracy. Additionally, we

observe at $p = 0.5$ that the oscillator strength in the limits of small and large magnetic fields is considerable only for two of the modes, except in the gap region, where three modes contribute. By comparison of Fig.s 3a and 4b we see that the magnetic field for minimum gap (between the second and third mode) increases with increasing p , whereas the gap width decreases. Consequently, the location and width of the gap provides information on the interaction strength.

By comparison of Fig.s 2 and 3 with Fig.4, and more clearly by consideration of formula (36) and Fig.5, it becomes clear that in either case the lower pair of degenerate modes at $B = 0$ converges to a constant (the mean square bare confinement frequency $\sqrt{(\omega_1^2 + \omega_2^2)/2}$, which amounts to $1.02 \omega_0$ in our numerical example). Even for finite B , there are two branches, which converge to a finite (B -dependent) value for $p \rightarrow \infty$, or in other words, which become independent of p in this limit. At first sight this looks surprising because the e e interaction does not show any saturation, if we increase the interaction parameter, but it continues to compress the dot state. However, there is a simple visual explanation for this feature: Generally, the dot interaction adds an additional second order contribution to the confinement, which has the same symmetry as the lattice, i.e. it is circular for a cubic lattice. For large p , this additional term outweighs the bare confinement, and the effective confinement in both dots becomes isotropic and equal. Thus, we approach the case of a lattice of identical dots, for which a pair of Kohn modes exists. Because these Kohn modes do not exactly agree with the modes of noninteracting dots, we call them *pseudo* Kohn modes. In a sense, the Generalized Kohn Theorem reentries for dot lattices with strong interdot interaction. In other lattices with lower symmetry, the effective confinement in the strong interaction limit might be elliptical, leading pseudo Kohn modes with a gap at $B = 0$. The other pair of modes (which diverge for $p \rightarrow \infty$) turns into the in-folded modes at the Brillouin zone corner (because the units cell halves if all dots become equivalent). These modes become spurious in the long wavelength and the large- p limit and the oscillator strength of them converge to zero.

In Fig.s 3a and 4b we observe an additional qualitative effect of dot interaction. For isolated elliptical dots we expect a gap between the two excitation branches at $B = 0$. However, for larger p only the pseudo Kohn mode might be observable, because the oscillator strength of the BZ boundary mode decrease rapidly. On the other hand, the two lower modes for finite p develop out of the degenerate lower mode for $p = 0$, whereby the degeneracy at $B = 0$ survives. Therefore, at $B = 0$ it looks as if we had a circular dot. The closing of the gap between the two most intensive branches at $B = 0$ is *not* a gradual effect proceeding with increasing p , but initiated by symmetry. (For a deeper understanding see also the additional figures in Ref. ?.)

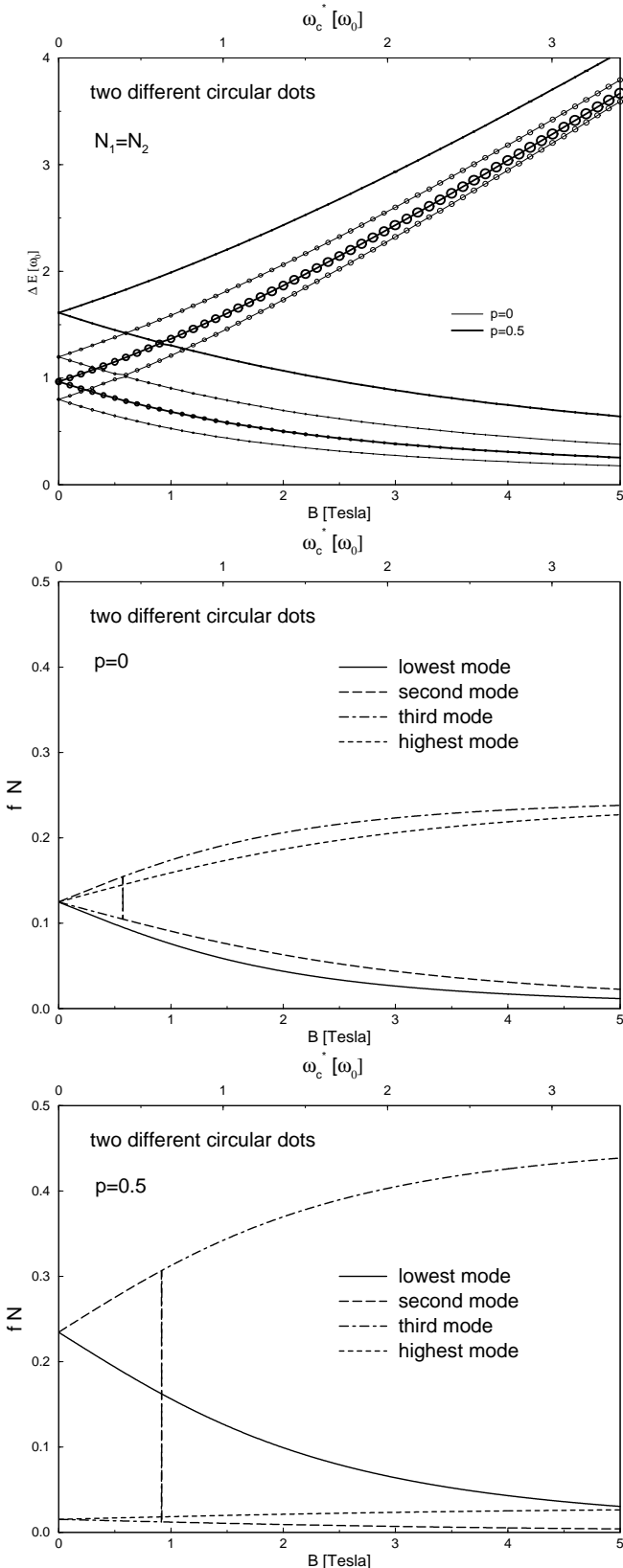


FIG. 2. Excitation modes (a) and oscillator strength (multiplied with N) for $p = 0$ (b) and $p = 0.5$ (c) for a lattice with two different circular dots as described in the text. The radius of the circles in (a) is proportional to the oscillator strength and provides a rough overview.

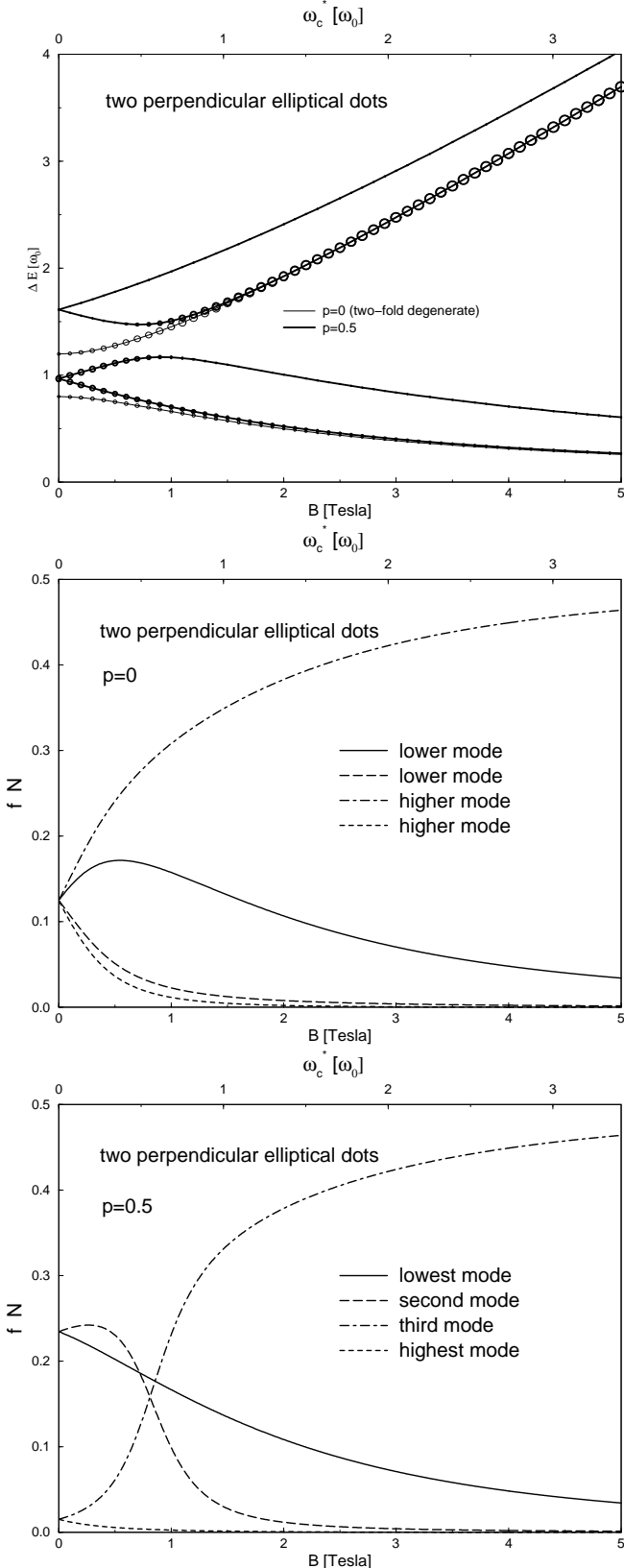


FIG. 3. Excitation modes (a) and oscillator strength (multiplied with N) for $p = 0$ (b) and $p = 0.5$ (c) for a lattice with two identical, but rotated elliptical dots as described in the text and shown in Fig.1. The radius of the circles in (a) is proportional to the oscillator strength and provides a rough overview.

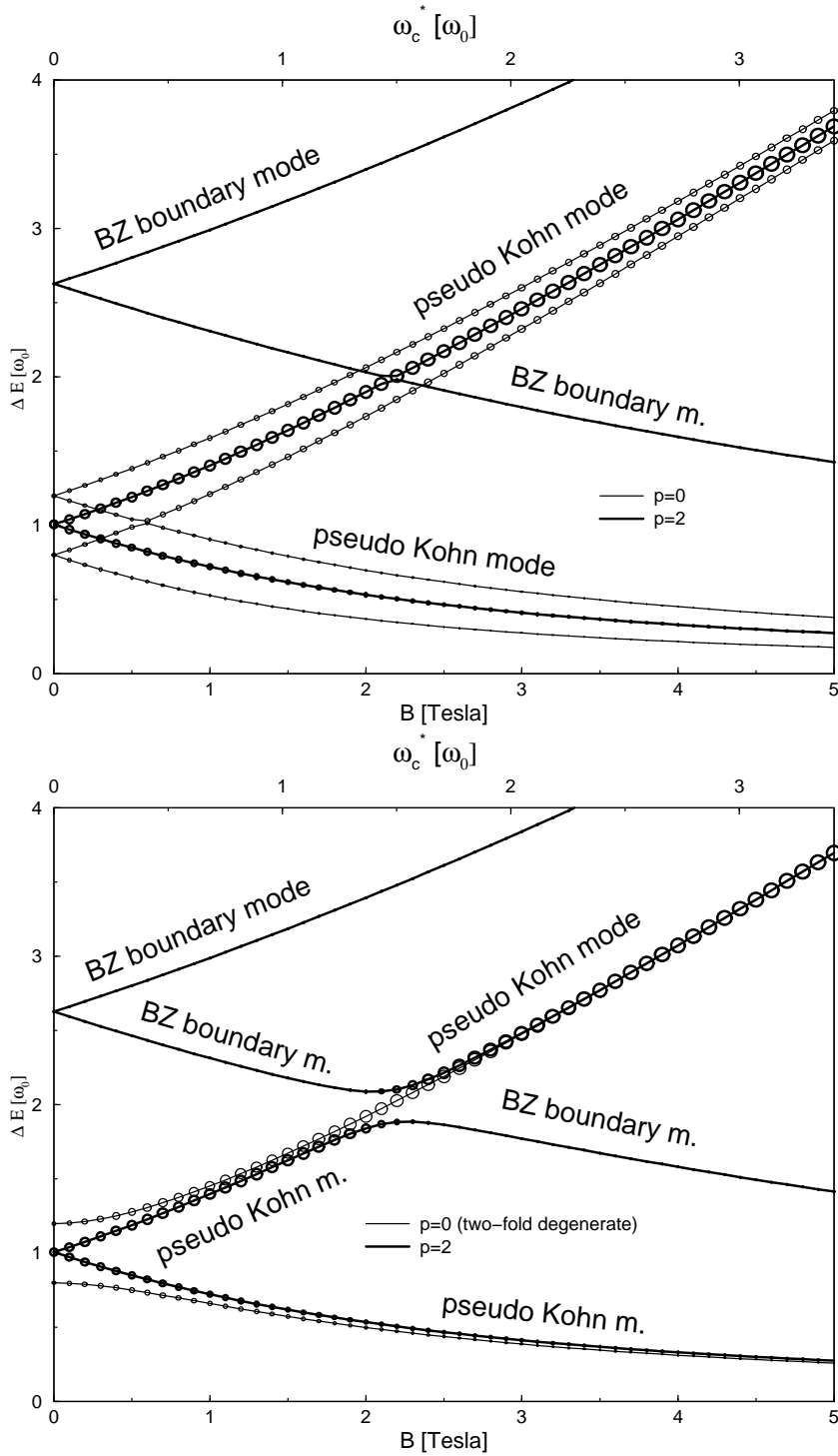


FIG. 4. Excitation modes for a lattice with two different circular dots (a) and two rotated elliptical dots (b) for a large interaction parameter ($p = 2$). The radius of the circles is proportional to the corresponding oscillator strength.

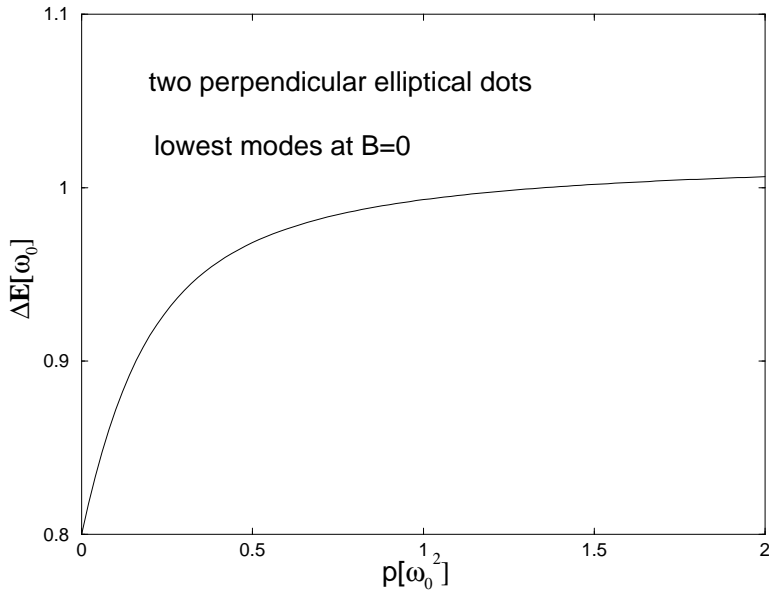


FIG. 5. Pseudo Kohn mode at $B = 0$ as a function of interaction parameter p for a lattice with two perpendicular elliptical dots per unit cell.

VI. SUMMARY

We have shown that breaking the GKTh by constructing quantum dot lattices with at least two different dot confinements per unit cell has experimentally observable consequences. Generally speaking, there are no Kohn modes, i.e. interaction independent modes, anymore. In both of the considered cases, the degeneracy in the FIR *intensities* at $B = 0$ between the upper and lower absorption lines is lifted due to dot interaction. For two mutually rotated elliptical dots (per cell), we observe also a splitting of formerly degenerate absorption *frequencies* and the appearance of an anticrossing. For two different circular dots no qualitative effect of e e interaction in the absorption frequencies is observed. Instead, the absorption spectrum can be mimiced by two noninteracting dots with modified (effective) confinements. We also pointed out that an extensively strong interaction destroys the effect of interaction by producing pseudo- Kohn modes. Although this limit cannot be reached experimentally, it might be important to take this tendency into consideration.

Only in the case of two circular dots there is a simple analytical closed form solution. However, with the formulae presented above, the absorption frequencies and oscillator strength for any cubic lattice with two harmonic dot species can be easily calculated. The only numerical task is to find the eigenvalues of an explicitly given non- Hermitian 8×8 matrix and to perform a special sum over the eigenvector components.

VII. ACKNOWLEDGMENT

I am indebted to D.Heitmann, J.Kotthaus, and H.Eschrig, and their groups, as well as G.Paasch for helpful discussion.

¹ W.Kohn, Phys.Rev. **123**,1242(1961); L.Brey,N.F.Johnson, and B.I.Halperin, Phys.Rev. B**40**,10647(1989); P.A.Maksym and T.Chakraborty, Phys.Rev.Lett. **65**,108(1990); F.M.Peeters, Phys.Rev. B**42**,1486(1990)

² M.Taut, cond. mat. 0002155 and accepted for Phys. Rev. B

³ D.Heitmann, K.Bollweg,V.Gudmundson,T.Kurth, and S.P.Riege, Physica E 1,204 (1997)

⁴ D.Pfannkuche, and R.Gerhardts, Phys.Rev. **44**, 13132 (1991)

⁵ T.Darnhofer, U.Rössler, and D.A.Broido, Phys. Rev. B **52**, 14376 (1995) ; Phys. Rev. B **53**,13631 (1996)

⁶ L.Jacak, P.Hawrylak, and A.Wojs, *Quantum Dots*, Springer 1998

⁷ J.Dempsey, N.F.Johnson, L.Brey, and B.I.Halperin, Phys.Rev. B **42**,11708 (1990)

⁸ C.Tsallis, J.Math.Phys. **19**, 277 (1978); Y.Tikoshinsky, J.Math.Phys. **20**,406 (1979)